

Total absorption by degenerate critical coupling

Jessica R. Piper, Victor Liu, and Shanhui Fan

Citation: [Applied Physics Letters](#) **104**, 251110 (2014); doi: 10.1063/1.4885517

View online: <http://dx.doi.org/10.1063/1.4885517>

View Table of Contents: <http://scitation.aip.org/content/aip/journal/apl/104/25?ver=pdfcov>

Published by the [AIP Publishing](#)

Articles you may be interested in

[Investigation of the graphene based planar plasmonic filters](#)

Appl. Phys. Lett. **103**, 211104 (2013); 10.1063/1.4831741

[Polarization-dependent optical absorption of graphene under total internal reflection](#)

Appl. Phys. Lett. **102**, 021912 (2013); 10.1063/1.4776694

[Triangular resonator with surface plasmon resonance around the critical angle](#)

J. Appl. Phys. **110**, 073107 (2011); 10.1063/1.3638710

[Influence of the cavity parameters on the output intensity in incoherent broadband cavity-enhanced absorption spectroscopy](#)

Rev. Sci. Instrum. **78**, 073104 (2007); 10.1063/1.2752608

[Terahertz cavity-enhanced attenuated total reflection spectroscopy](#)

Appl. Phys. Lett. **86**, 201116 (2005); 10.1063/1.1929072



AIP | Journal of
Applied Physics

Journal of Applied Physics is pleased to
announce **André Anders** as its new Editor-in-Chief

Total absorption by degenerate critical coupling

Jessica R. Piper,^{a)} Victor Liu, and Shanhui Fan^{b)}

Ginzton Laboratory, Department of Electrical Engineering, Stanford University, Stanford, California 94305, USA

(Received 29 April 2014; accepted 16 June 2014; published online 24 June 2014)

We consider a mirror-symmetric resonator with two ports. We show that, when excited from a single port, complete absorption can be achieved through critical coupling to degenerate resonances with opposite symmetry. Moreover, any time two resonances with opposite symmetry are degenerate in frequency and absorption is always significantly enhanced. In contrast, when two resonances with the same symmetry are nearly degenerate, there is no absorption enhancement. We numerically demonstrate these effects using a graphene monolayer on top of a photonic crystal slab, illuminated from a single side in the near-infrared. © 2014 AIP Publishing LLC.

[<http://dx.doi.org/10.1063/1.4885517>]

The possibility of achieving 100% absorption in a one-port resonator configuration by critical coupling is well known.^{1–4} An example of such a one-port is shown in Figure 1(a). The green region represents a resonant optical structure with some dissipative loss, which is backed by a perfect mirror. A normally incident wave will be reflected back along the same path; then the front face of the resonator constitutes the only port the resonator couples to. When the leakage rate of energy out of the resonator is equal to the dissipation rate in the resonator, all of the incident power will be absorbed on resonance: this is the condition of *critical coupling*.¹ In recent years, the concept of *coherent perfect absorption*^{5,6} has been developed, as a generalization of critical coupling, where complete absorption can be achieved in a two-port when light is incident from both ports with a specific linear combinations of the incident amplitudes in the ports.

In this Letter, we consider the condition for total absorption in a mirror-symmetric two-port resonator configuration, when light is incident into one of the ports only. Figure 1(b) shows a schematic of a two-port optical resonator. Now we can access the system from both sides, so for normal incidence, each face of the resonator acts as a port. The mirror plane of the system is perpendicular to the plane of incidence, as indicated by the dashed line in the figure. If the resonator supports a single resonance, then at most 50% of the incident power can be absorbed when the system is illuminated from a single side, as we show in the following paragraphs. However, an input beam from a single side can be completely absorbed in such a two-port resonator configuration, provided that the resonator supports two resonances which are *degenerate* in frequency but have *opposite* symmetry with respect to the mirror plane of the system, and the leakage rate of energy out of the resonator for each resonance is equal to the dissipation rate for that resonance (i.e., each resonance is critically coupled). We call this phenomena *degenerate critical coupling*.

The requirement of two opposite-symmetry resonances to achieve total absorption can be understood from a symmetry argument. The eigenexcitations of a mirror-symmetric

system are even and odd combinations of equal-amplitude waves at the two input ports; the modes of the resonator are also even or odd. Suppose a resonator supports a single even mode: then only the even eigenexcitation can couple to this mode. If the even resonance is critically coupled, then all input power can be absorbed when the system is illuminated coherently with the even eigenexcitation. For the same resonator supporting a single even resonance, if instead we have a beam incident from a single side, the incident beam can be decomposed into an equal magnitude linear combination of the even and odd eigenexcitations. Since the odd eigenexcitation does not excite the resonance, it follows that at most only 50% of the power can be resonantly absorbed.⁷ Therefore, we see that to accomplish 100% resonant absorption in a symmetric two-port system with light incident from one side, the system must support degenerate resonances with opposite symmetry, and each resonance is required to be critically coupled.⁸

We use coupled mode theory to derive the conditions for total absorption by degenerate critical coupling. We consider the behavior of a mirror symmetric resonator which supports two resonances and which communicates with the outside world via two identical ports. Each port supports incoming and outgoing waves. If the resonator is lossless and has time reversal symmetry, then we can describe its behavior by⁹

$$\dot{a} = i(\Omega + i\Gamma)a + D^T u, \quad (1)$$

$$y = Cu + Da. \quad (2)$$

Here, $a \in \mathbb{C}^2$ is the vector of complex mode amplitudes, with $|a_j|^2$ giving the energy stored in mode j ; Ω and Γ are real 2×2 symmetric matrices, giving the rates of phase change and amplitude change of the resonances, respectively; $u \in \mathbb{C}^2$ gives the input amplitude at each port, with $|u_j|^2$ being the incident power in port j , and y likewise represents the output amplitudes; C is the background scattering matrix, which gives the reflection and transmission between the ports in the absence of the resonator, with $C^H C = 1$ (where C^H represents the conjugate transpose of C); and the matrix D gives the coupling between the resonator modes and the ports.

^{a)}jrylan@stanford.edu

^{b)}shanhui@stanford.edu

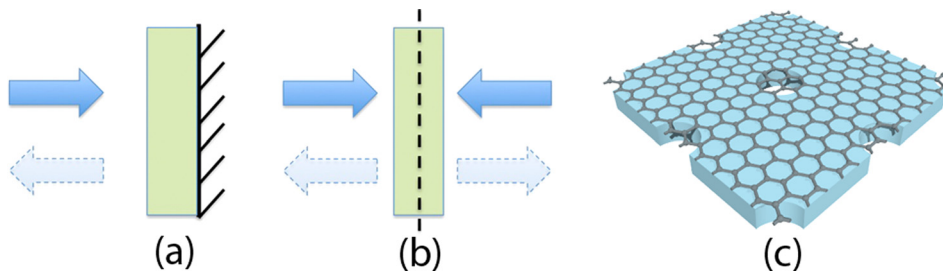


FIG. 1. (a) Schematic of a resonator system (green region) with one port. The backside of the resonator is a perfect mirror. (b) Schematic of a resonator system with two ports. The system has a mirror plane symmetry indicated by the dashed line. (c) A resonator system consisting of a graphene layer (gray, not to scale) placed on top of a photonic crystal slab (light blue).

The operator $\Omega + i\Gamma$ is not Hermitian, so, in general, its eigenvalues will be complex. However, if the resonances have opposite symmetry properties, we can simultaneously diagonalize Ω , Γ , and D , with $D^2 = 2\Gamma$. Then the diagonal terms ω_j give the natural frequency of each resonance, while γ_j give the leakage rate of each resonance to the ports. For steady-state input from a single port with unit amplitude at frequency ω , the energy stored in the resonator is a sum of Lorentzian terms

$$|a|^2 = \sum_{j=1}^2 \frac{\gamma_j}{(\omega - \omega_j)^2 + \gamma_j^2}. \quad (3)$$

Note that the energy storage in the resonator is independent of the background reflection and transmission coefficients given by C .

As we add dissipative loss to the system, in general, we expect that the resonances will no longer be orthogonal. However, if the loss does not change the underlying symmetry of the structure, and so the loss due to the each resonance remains independent, then we can modify Eq. (1) to $\dot{a} = i(\Omega + i\Gamma + i\Delta) + D^T u$, where Δ is real and diagonal, with elements $\delta_j > 0$ giving the modal dissipation rate. We can still apply Eq. (3) to find the stored energy in the system with loss by replacing the term γ_j^2 in the denominator with $(\gamma_j + \delta_j)^2$. Under excitation from a single port, the absorption in the system is given by

$$A = \sum_{j=1}^2 \frac{2\delta_j\gamma_j}{(\omega - \omega_j)^2 + (\gamma_j + \delta_j)^2}, \quad (4)$$

where we note that the absorption is independent of the background reflection and transmission coefficients given by the C matrix. While the transmission spectrum of such a system can exhibit an asymmetric Fano lineshape, the absorption spectrum will be a sum of symmetric Lorentzian lineshapes.

Each term in the sum will attain a maximum of 0.5 when $\omega = \omega_j$, $\gamma_j = \delta_j$. This is the condition for critical coupling for a single resonance. If the resonances are far apart ($|\omega_1 - \omega_2| \gg \gamma_j$), then at any given frequency only one term contributes, and we have a maximum absorption of 50%, as we arrived at before from a symmetry argument. On the other hand, for the case where $\omega_1 = \omega_2$, $\delta_1 = \gamma_1$, and $\delta_2 = \gamma_2$, both resonances will be critically coupled, and we will have total absorption. This is the condition for *degenerate critical coupling*. Moreover, as can be seen by Eq. (4), there will always be absorption enhancement any time two resonances with opposite symmetry cross, even if neither resonance is critically coupled.

It has previously been demonstrated that a lossless, mirror-symmetric photonic crystal slab with background transmission $|t| = 1$ and two resonances with opposite

symmetry that are degenerate in both frequency *and* leakage rates can be used to construct an all-pass filter.¹⁰ The degenerate critical coupling condition for complete absorption derived here is related to the conditions for an all-pass filter, but differs in two significant aspects: there are no requirements on the background reflection and transmission, and we do not require the leakage rates of the two resonances to be the same.

We contrast the concept of degenerate critical coupling developed in this work, with the concept of coherent perfect absorbers.^{5,6} A two-port coherent perfect absorber is described by a 2×2 scattering matrix with a one-dimensional null space. In contrast, in a two-port satisfying the condition of degenerate critical coupling, the scattering matrix has two 0 eigenvalues, and hence a two-dimensional null space. Any linear combination of the incident amplitudes from the two ports is completely absorbed.

As an illustration of the theoretical considerations presented above, we consider a photonic crystal slab in air, with a graphene monolayer deposited on one side, as illustrated schematically in Figure 1(c). The slab by itself has mirror symmetry in the out-of-plane direction. The graphene adds dissipation to the system, but it is so thin that it barely breaks the mirror symmetry. The photonic crystal slab is made from a thin sheet of silicon with cylindrical air holes of constant radius on a square grid. Photonic crystal slabs support guided resonances, which are quasi-bound states with their in-plane wavevector k_{\parallel} overlapping those of the continuum of radiation modes.^{11–14} When excited on resonance, photonic crystal slabs exhibit significant local field enhancement and energy storage.

In our calculations, the photonic crystal slab is characterized by its thickness d , its lattice constant Λ , and its hole radius r . In the present work, we use the slab thickness as a variable to enable resonance crossing, but one may also vary the angle of incidence for a fixed structure. All simulations were performed using the S^4 implementation¹⁵ of the rigorous coupled wave analysis¹⁶ method. This is a fully vectorial method for numerically solving Maxwell's Equations. We used $n = 3.52$ for the refractive index of silicon, appropriate for the near-infrared wavelength range. The graphene has thickness of 0.34 nm, with refractive index given by $n = 3 + j5.446\lambda/3$, with λ in μm , as appropriate for undoped graphene in the visible and near-infrared.¹⁷

In Figure 2, we show the absorption of the system shown schematically in Figure 1(c) as a function of frequency and slab thickness, under plane wave illumination from one side at normal incidence. In this plot, the photonic crystal has $\Lambda = 1 \mu\text{m}$, and $r = 0.19 \mu\text{m}$. Away from resonance (black regions in Fig. 2(a)), the absorption background can be

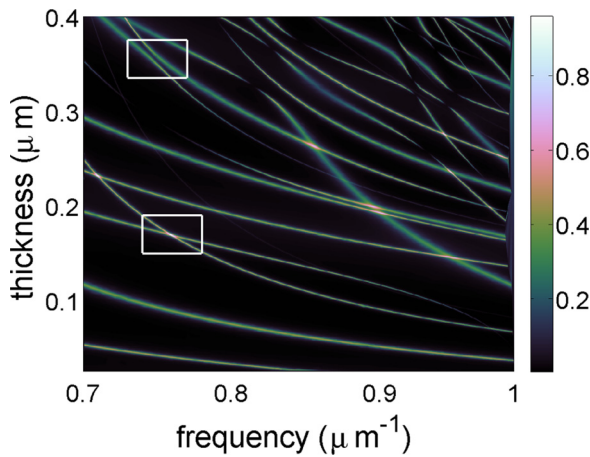


FIG. 2. Absorption versus frequency and photonic crystal slab thickness, for the structure shown in Figure 1(c). The photonic crystal slab has lattice period $\Lambda = 1 \mu\text{m}$, and radius $r = 0.19 \mu\text{m}$. The white boxes enclose a crossing near the frequency of $0.76 \mu\text{m}^{-1}$ with $d = 170 \text{ nm}$, and an anti-crossing near the frequency of $0.75 \mu\text{m}^{-1}$ with $d = 350 \text{ nm}$.

suppressed to below 1%. As is well known, a graphene sheet in air absorbs 2.3% of incident light in the visible and near infra-red at normal incidence.¹⁸ The various physical mechanisms that give rise to similar absorption suppression have recently been discussed.^{19,20} We observe lines in Figure 2 where the absorption is greatly enhanced over the background; these lines represent the resonances in the structure. For single resonances, which are isolated from other resonances, the absorption is typically less than 50%. At each crossing of two resonances with opposite symmetry, the absorption is significantly enhanced. In contrast, resonances with the same symmetry exhibit anti-crossing behavior, and there is no additional absorption enhancement near the anti-crossing point.

We reach the optimal structure through a search in a three-dimensional space of parameters including frequency, thickness of the slab, and the radius of the holes. While reaching the structure with near complete absorption discussed in this Letter did involve a detailed search, the physics of absorption enhancement due to crossing of modes with opposite symmetry is readily observed in a large number of structures. As a result, a significant fraction of the structures examined support graphene absorption that is substantially above 50% at some frequencies. For the remainder of this Letter, we will focus on the crossing near the frequency of $0.76 \mu\text{m}^{-1}$ ($\lambda = 1.32 \mu\text{m}$) for a slab around 170 nm thick, and the anti-crossing near the frequency of $0.75 \mu\text{m}^{-1}$, for a slab around 350 nm thick, both of which are outlined in white in Figure 2.

Figure 3(a) shows the absorption in the graphene layer as a function of frequency and thickness of the photonic crystal slab, in a close-up around the resonance crossing highlighted in Figure 2. The peak absorption of 98% occurs at the frequency of $0.759 \mu\text{m}^{-1}$ ($\lambda = 1.32 \mu\text{m}$) for the slab thickness $d = 169 \text{ nm}$. The linewidth of the absorption peak is 6 nm, and the Q is around 170. Figures 3(d) and 3(e) show the distribution of the in-plane electric field magnitude $|E_{\parallel}|^2$ at the degenerate resonances in transverse cuts along the edge of the unit cell. The even resonance in Figure 3(d) has an antinode along the centerline of the photonic crystal slab,

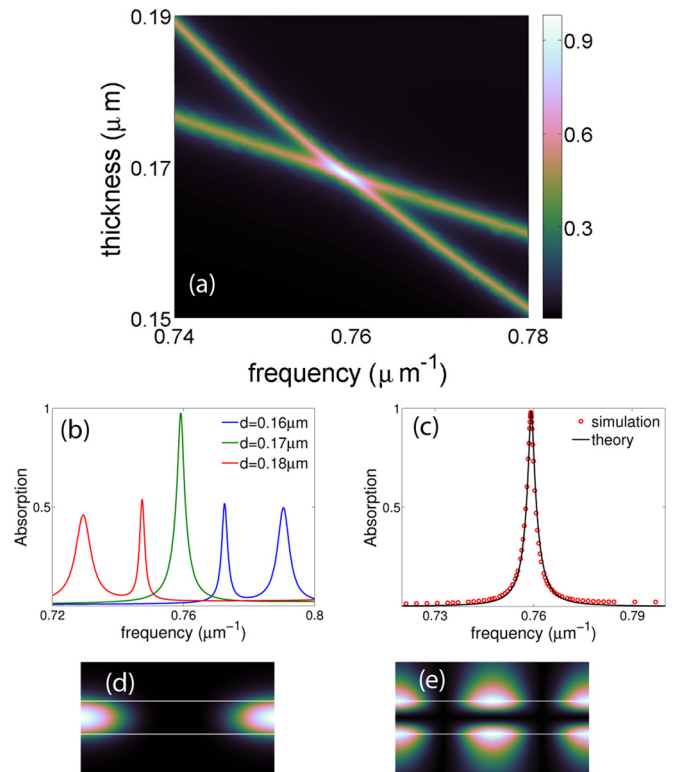


FIG. 3. (a) Absorption enhancement at crossing of two resonances with opposite symmetry, as a function of frequency and photonic crystal slab thickness. The even resonance has a steeper slope in the plot. (b) Absorption enhancement below, at, and above the crossing of two resonances with opposite symmetry. Away from the degeneracy, each resonance has a maximum absorption of around $A = 0.5$. When the resonances are degenerate, we have $A = 0.98$. (c) Coupled mode theory analysis of enhanced absorption at crossing of two resonances with opposite symmetry. The excellent agreement between the simulation data and the theory calculation validates our use of coupled mode theory. Panels (d) and (e) show the distribution of $|E_{\parallel}|^2$ in transverse cuts along the edge of the unit cell. Panel (d) shows the even resonance, while panel (e) shows the odd resonance.

while the odd resonance in Figure 3(e) has a nodal plane there, and stores more of its energy in the air outside the slab. Therefore, the dissipation rates of the even and odd mode can differ significantly, allowing for the possibility of degenerate critical coupling.

The absorption spectra for three slab thicknesses near 170 nm are shown in Figure 3(b). Away from the degeneracy, each resonance has a peak absorption of around 50%, while at the degeneracy the absorption of each resonance sums, as predicted by Eq. (4). The absorption at the degenerate resonance is compared to our degenerate coupled mode theory in Figure 3(c). The leakage and dissipation rates γ_j , δ_j were obtained by fitting the stored energy in the photonic crystal resonator with and without graphene, respectively, using Eq. (3). The absorption was then calculated using Eq. (4). The results of the degenerate coupled mode theory agree excellently with the numerically calculated absorption spectrum.

The resonant frequencies of the even (odd) mode without graphene are 0.7593 (0.7594) μm^{-1} ; with graphene the resonant frequencies shift to 0.7592 (0.7591) μm^{-1} . The leakage rates γ are 0.49 (15.2) nm^{-1} , while the dissipation rates δ are 0.51 (11.0) nm^{-1} . The residual 2% scattering, which is accurately captured by the coupled mode theory

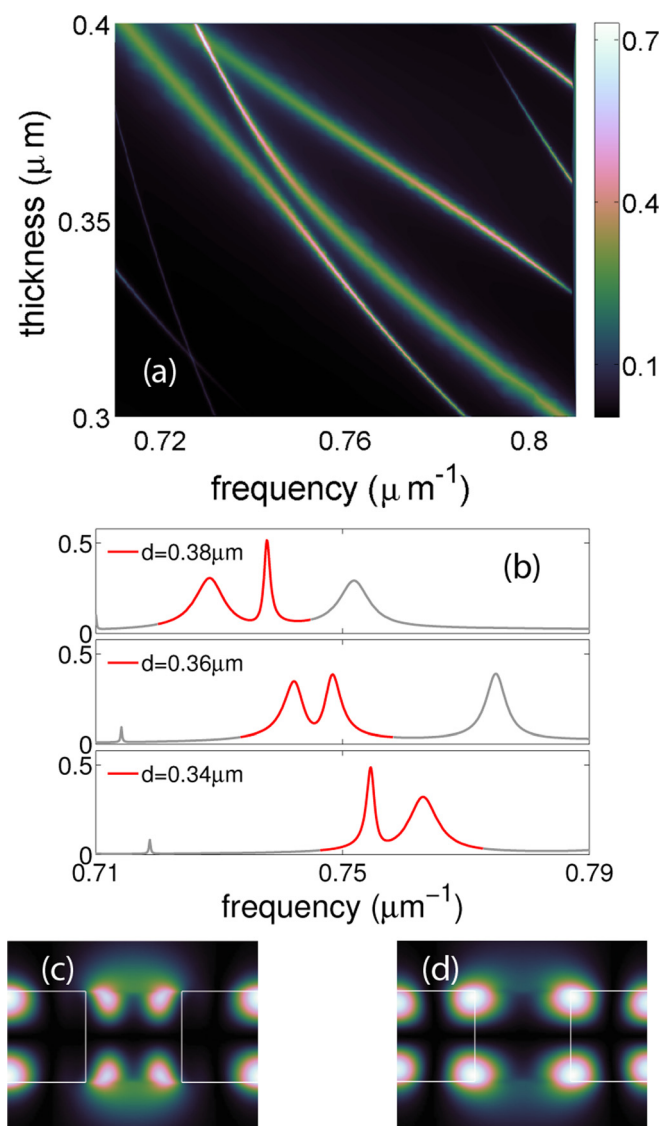


FIG. 4. (a) Absorption in the vicinity of an anti-crossing of two resonances with the same symmetry, as a function of frequency and photonic crystal slab thickness. (b) Absorption spectra for three photonic crystal slab thicknesses. The sections of the spectra containing the anti-crossing resonances are shown in red. The exchange of line shapes in the spectra for the thickest and the thinnest slab is a signature of anti-crossing. Panels (c) and (d) show the distribution of $|E_{||}|^2$ along transverse cuts through the centerline of the unit cell. Both resonances have odd symmetry.

calculation, is due primarily to the imperfect critical coupling of the odd resonance, and imperfect degeneracy, rather than symmetry breaking by the graphene.

In Figure 4(a), we show the absorption in the graphene in the vicinity of the resonance anti-crossing highlighted in Figure 2, near the frequency of $0.746\mu\text{m}^{-1}$. The anti-crossing resonances are closest in frequency for a slab thickness of $d = 356\text{ nm}$. The profiles of $|E_{||}|^2$ for the two resonances in transverse cuts through the centerline of the photonic

crystal slab are shown in Figures 4(c) and 4(d). Both modes are clearly odd, as indicated by the nodal plane at the center of the photonic crystal slab in the transverse cuts. We show the absorption spectra for several thicknesses around $d = 356\text{ nm}$ in Figure 4(b). The sections of the spectra containing the anti-crossing resonances are shown in red. In the vicinity of the anti-crossing, there is no additional absorption enhancement beyond what a single resonance can provide.

The mechanism of *degenerate critical coupling* could be readily applied to several important applications. First, one could construct of a perfect absorber with thickness much smaller than a wavelength, without requiring the use of a mirror, which could be important for photodetector applications. Second, the graphene in our system could be gated by applying an electrostatic potential, in order to tune the system in and out of resonance, creating a tiny, high-contrast transmission modulator. Finally, the mechanism of degenerate critical coupling could be applied to other ultra-thin films, and other types of lossy optical resonators.

This work was supported in part by an AFOSR-MURI program (Grant No. FA9550-12-0024). J.R.P. was additionally supported by the Robert and Ruth Halperin Stanford Graduate Fellowship. We also acknowledge discussion with Professor L. Cao and co-workers on their unpublished work.⁸

¹H. A. Haus, *Waves and Fields in Optoelectronics* (Prentice-Hall, Englewood Cliffs, NJ, 1984).

²A. Yariv, *IEEE Photonic Technol. Lett.* **14**, 483 (2002).

³J. R. Tischler, M. S. Bradley, and V. Bulović, *Opt. Lett.* **31**, 2045 (2006).

⁴J. R. Piper and S. Fan, *ACS Photon.* **1**, 347 (2014).

⁵Y. Chong, L. Ge, H. Cao, and A. D. Stone, *Phys. Rev. Lett.* **105**, 053901 (2010).

⁶W. Wan, Y. Chong, L. Ge, H. Noh, A. D. Stone, and H. Cui, *Science* **331**, 889 (2011).

⁷L. C. Botten, R. C. McPhedran, N. A. Nicorovici, and G. H. Derrick, *Phys. Rev. B* **55**, R16072 (1997).

⁸L. Huang, Y. Yu, and L. Cao, e-print arXiv:1404.6842.

⁹W. Suh, Z. Wang, and S. Fan, *IEEE J. Quantum Electron.* **40**, 1511 (2004).

¹⁰W. Suh and S. Fan, *Appl. Phys. Lett.* **84**, 4905 (2004).

¹¹V. Astratov and I. Culshaw, *J. Lightwave Technol.* **17**, 2050 (1999).

¹²T. Tamir and S. Zhang, *J. Opt. Soc. Am. A* **14**, 1607 (1997).

¹³S. Fan and J. Joannopoulos, *Phys. Rev. B* **65**, 235112 (2002).

¹⁴W. Zhou, D. Zhao, Y.-C. Shuai, H. Yang, S. Chuwongin, A. Chadha, J.-H. Seo, K. X. Wang, V. Liu, Z. Ma, and S. Fan, *Prog. Quantum Electron.* **38**, 1 (2014).

¹⁵V. Liu and S. Fan, *Comput. Phys. Commun.* **183**, 2233 (2012).

¹⁶M. G. Moharam and T. K. Gaylord, *J. Opt. Soc. Am.* **71**, 811 (1981).

¹⁷M. Bruna and S. Borini, *Appl. Phys. Lett.* **94**, 031901 (2009).

¹⁸R. R. Nair, P. Blake, A. N. Grigorenko, K. S. Novoselov, T. J. Booth, T. Stauber, N. M. R. Peres, and A. K. Geim, *Science* **320**, 1308 (2008).

¹⁹H. Fang, H. A. Bechtel, E. Plis, M. C. Martin, S. Krishna, E. Yablonovitch, and A. Javey, *Proc. Natl. Acad. Sci. U.S.A.* **110**, 11688 (2013).

²⁰K. X. Wang, J. R. Piper, and S. Fan, *Nano Lett.* **14**, 2755 (2014).